Conformation of isotactic polystyrene (IPS) in the bulk crystallized state as revealed by small-angle neutron scattering

Jean Michel Guenet and Claude Picot

Centre de Recherches sur les Macromolécules, C.N.R.S., 6 rue Boussingault, 67083 Strasbourg Cedex, France

Neutron scattering experiments have been performed on isotactic polystyrene (IPS) samples in the bulk crystallized state ($T_{crystallization}$ = 185°C). The determination of the conformation of tagged chains ranging from 2.5 x 10^5 to 7 x 10^5 has been undertaken on two different hydrogenated IPS matrices. A matrix of usual molecular weight (M_w = 4 x 10^5) leads to results which do not agree with Flory's model. In this case, measurements on radius of gyration R_g show on the one hand an important increase of this parameter (~40%) with increasing crystallinity for the highest molecular weight tagged chains and on the other hand a variation with molecular weight like $M^{0.78}$. These results are interpreted with a schematic model involving a long crystalline sequence incorporated in the monocrystal along the 110 plane and two amorphous wings. Such an assumption is confirmed by the scattering behaviours in the intermediate range. On the other hand, by using an IPSH matrix of very high molecular weight (M_w = 1.75 x 10^6), and the same tagged chains previously considered, a very weak variation of R_g with increasing crystallinity is observed. This leads to consider in this case Flory's conformation which is corroborated by data obtained in the intermediate range.

INTRODUCTION

Small-angle neutron scattering (SANS) has allowed successful determination of the conformations of polymer chains in the glassy state, of rubbers and of concentrated solutions[1–3]. For crystallizable polymers SANS results have shown that the chains behave in a Gaussian-like manner above their melting point[4,5]. However, many difficulties arise in the interpretation of neutron scattering data for some polymers in the bulk-crystallized state. The problems arise from the difference of crystallization growth rate between deuterated and protonated species leading to the formation of molecular clusters. This has been reported in particular by Schelten *et al.* on polyethylene[6] and by Allen and Tanaka on poly(ethylene oxide)[7]. Nevertheless, the clustering phenomenon generally vanishes for polyethylene when the samples are fast quenched from the molten state to room temperature. The degree of crystallinity then reaches a value close to 65%. SANS experiments performed on such systems[8,9] coupled with form factor calculations[10] would lead to assume globally crystallized chains passing through several monocrystals. The number of consecutive foldings of a chain in the same lamella would not be larger than 3. As yet, it seems that such an interpretation is not universally accepted. Ullman *et al.*[11] suggest that results obtained from SANS measurements on polyethylene are not really correctly treated since the background which should be removed from the total scattering cross-section does not correspond necessarily to that measured on a totally hydrogenated sample.

Such considerations lead us to investigate another crystallizable polymer. Isotactic polystyrene (IPS) has been chosen for several reasons. Though IPS cannot reach a very high crystallinity rate, this parameter is easily controlled by annealing amorphous samples for different times. Then a SANS study as function of degree of crystallinity can be performed giving information on the evolution of the chain conformation. The polymer is also available by fractionation with narrow molecular weight distribution as detailed in a previous paper[12]. It must be mentioned that the background effect described earlier is negligible provided that the concentration of D-species is weak (~1%). Finally, as it will be shown later, segregation between hydrogenated and deuterated macromolecules does not take place during the crystallization of this polymer.

EXPERIMENTAL

Materials

Hydrogenated (IPSH) and deuterated (IPSD) polymers have been synthesized following the well known Natta method[13]. The description of synthesis, purification, fractionation and tacticity measurements achieved on these samples is available in ref 12. Blends of IPSH and IPSD have been obtained from solutions in dichlorobenzene precipitated in methanol (M_{WIPSH} = 4 x 10^5 with M_w/M_n ~ 1.4). Initially amorphous solid samples of 1 mm thickness have been moulded above melting temperature (~250°C) and quenched. Secondly, these samples have been annealed under vacuum in the mould for different times at a given temperature (185°C). The correspondence between degrees of crystallinity and annealing times is given in *Figure 1*. Crystallinities have been determined from density measurements assuming the non-existance of micro-voids. This point will be confirmed afterwards by SANS experiments.

0032–3861/79/121483–09$02.00

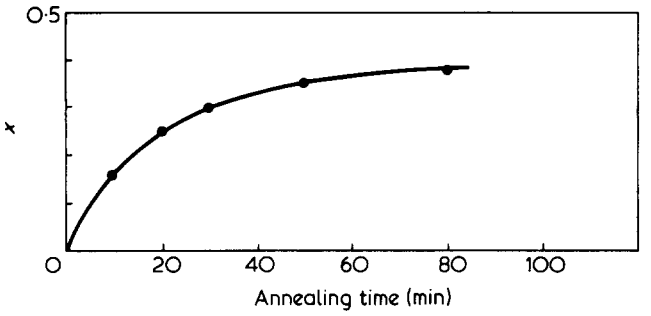

Figure 1 Crystallinity x against annealing time. Curve obtained at 185°C

Neutron scattering

All the experiments described in this paper have been performed on D11 and D17 scattering apparatus[14] available at the Institut Laue-Langevin in Grenoble (France). The scattering vectors $q = (4\pi/\lambda) \sin\theta/2$ were in the range:

$$5 \times 10^{-3} \leqslant q \leqslant 1.5 \times 10^{-2} \text{ Å}^{-1} \text{ for D11}$$

$$2 \times 10^{-2} \leqslant q \leqslant 7 \times 10^{-2} \text{ Å}^{-1} \text{ for D17}$$

Calibration measurements: determination of the eventual presence of clusters and micro-voids

As mentioned in the Introduction, the study of crystalline polymers by SANS is not a simple problem. One is no more dealing with a continuous medium as in the case of amorphous polymers or solutions. Four kinds of entities could be present in the medium: the residual amorphous material; the crystalline material; the micro-voids; the molecular clusters.

Ullman and coworkers have performed calculations[15] of the scattering cross-section of crystallized polymer which is heterogeneous in composition using a simple picture of a material composed of mosaic subunits each of which is large with respect to the neutron wavelength and is internally homogeneous. This effect is then characterized by a single parameter $\delta^2 = \overline{C_D^2} - \overline{C_D}^2$ describing the fluctuations in concentration of the D-species. By introducing this new parameter, the total intensity scattered by a blend of D- and H-species can be written according to these authors:

$$I_T(q) = K\{(a_H c_H + a_D c_D)^2 S_0(q) + \delta^2 (a_H - a_D)^2 S'_0(q) + S_{inc} + I(q)\} \quad (1)$$

where $C_D + C_H = 1$ and a are the scattering lengths. The term $I(q)$ is directly related to the shape of the labelled macromolecules, namely:

$$I(q) = (a_H - a_D)^2 MCP(q) \quad (2)$$

M being the molecular weight and C the concentration of the D-species in g/ml. $P(q)$ is a classical form factor. The background measured on an hydrogenated crystallized sample is given by:

$$I_0(q) = K[a_H^2 S_0(q) + S_{inc}] \quad (3)$$

where $S_0(q)$ and S_{inc} are respectively the coherent and incoherent cross-sections of the background.

For IPS, we must first consider the term $(a_H C_H + a_D C_D)^2$ in relation (1). By using concentrations of D-species of about 1% we obtain:

$$(a_H C_H + a_D C_D)^2 = (0.99 \times 2.32 + 0.01 \times 10.7)^2 \times 10^{-24} = 5.78 \times 10^{-24} \text{ cm}^2 \quad (4)$$

Knowing $a_H^2 = 5.38 \times 10^{-24}$ cm^2, the relative ratio r^2 is:

$$r^2 = \frac{a_H^2}{(a_H C_H + a_D C_D)^2} = 0.93 \quad (5)$$

This result has to be compared to the equivalent one for polyethylene:

$$r^2 = 0.65 \quad (6)$$

Then taking into account this small descrepancy in the case of IPS, relation (1) can be approximated as:

$$I_T(q) = K\{a_H^2 S_0(q) + \delta^2 (a_H - a_D)^2 S_0(q) + S_{inc} + I(q)\} \quad (7)$$

Such approximation is valid also for polyethylene in the Guinier range of scattering vectors where $I_T(q)$ is rather important with respect to $I_0(q)$, but could lead to erroneous results at wide q.

Much of $S_0(q)$ in relation (3) arises from micro-voids. In a continuous medium, $S_0(q)$ should be constant. In fact, this is the case in SANS for crystalline samples in a certain range of q (*Figure 2*) since densities of crystallized and amorphous chains are very close. Otherwise one would observe Bragg-peak. For example by introducing methyl ethyl ketone in a crystallized hydrogenated sample one can see in *Figure 2* a Bragg-peak due to the change in contrast factor between the crystalline and the amorphous-MEK phases. It is interesting to note that from this peak which corresponds to the long-spacing (d = 197 Å), one is able to estimate the lamellar thickness l_c. Since no change in dimensions of the sample (i.e. no swelling) has been observed by introducing MEK and knowing the linear crystallinity[16] which is close to 0.52, one finds $l_c \sim 100$ Å. Such result agrees with X-ray measurements performed on IPS samples crystallized at 185°C by several authors[17].

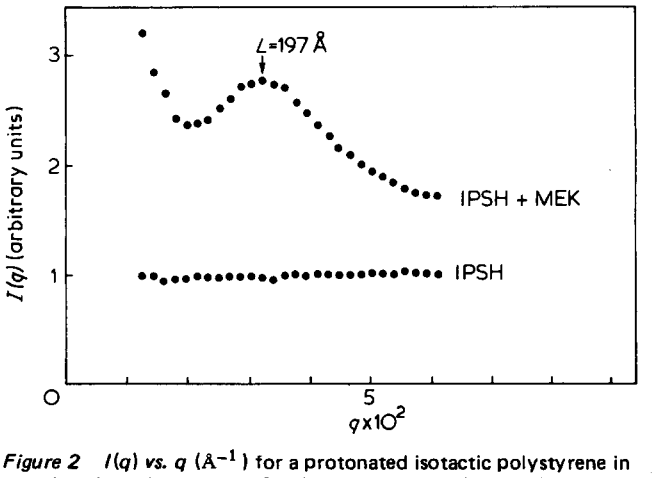

Figure 2 $I(q)$ *vs.* q (Å^{-1}) for a protonated isotactic polystyrene in two situations: lower curve for the scattering by the sample in the dry state, upper curve for scattering after introducing methyl ethyl ketone (MEK)

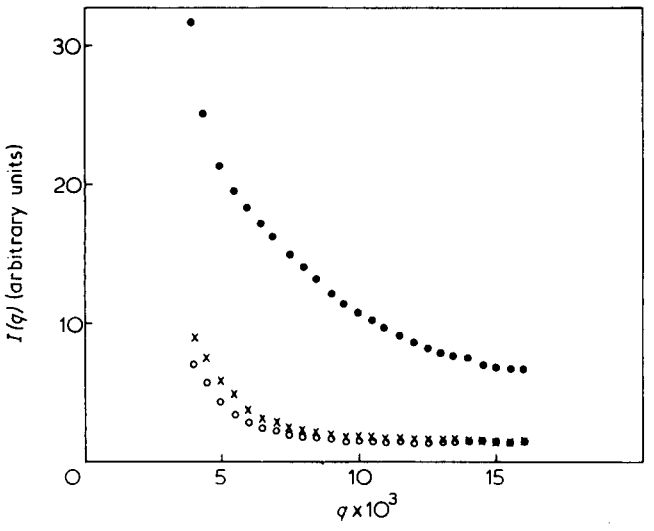

Figure 3 $I(q)$ *vs.* q (Å^{-1}). ●, Blend of H- and D-species (C = 0.51 × 10^{-2} g/ml; x, protonated 0.35-crystallized sample; ○, protonated amorphous sample

However, in the Guinier range of q, $S_0(q)$ does not remain constant but increases monotonously. This can be due to large micro-voids. In the case of IPS samples that have been investigated, the comparison between H-backgrounds of amorphous and crystallized samples shows only a small difference (*Figure 3*). The increase of intensity at low q can then be attributed to the direct beam contamination. On the same Figure is plotted the intensity scattered by a crystalline blend of H- and D-species (C_D = 0.51%) showing that coherent scattering of deuterated chains is rather important with respect to the background.

Let us now examine the term δ^2 which results from the contribution of eventually segregated tagged chains. To verify that the clustering phenomenon pointed out in polyethylene is non-existent, one has to determine the molecular weight from SANS experiments. This has been achieved using a method[18] proposed by Ullman. Knowing the hydrogenated background which becomes constant for wide q, one can roughly determine the apparatus constant K from relation (3)[19]. The SANS data yield:

$$M_w^{SANS} = 650\,000$$

whereas light scattering and g.p.c. experiments give:

$$M_w^{LS} = 559\,000 \qquad M_w^{g.p.c.} = 540\,000$$

Taking into account the relative accuracy of the molecular weight determination, particularly at low q one concludes that the clustering phenomenon can be ignored for IPS. This leads to $\delta^2 = 0$, and the background measured on a protonated sample can be subtracted from the intensity scattered by a mixture of hydrogenated and labelled chains in order to get directly $I(q)$.

SANS results

As clustering does not take place during IPS crystallization process, SANS data interpretation provides information on the conformation of isolated tagged chains imbedded in the semi-crystalline medium and the evolution of the macromolecule shape can be studied both as function of the molecular weight and the degree of crystallinity.

In the Guinier range of scattering vectors ($qR_g \ll 1$) $P(q)$ is approximated:

$$P(q) = 1 - q^2R_g^2/3 \tag{8}$$

The initial slope of $I^{-1}(q)$ *vs.* q^2 leads to the value of R_g^2. In *Figure 4* are plotted the variation of $I^{-1}(q)$ for the same labelled isotactic polymer ($M_w = 5 \times 10^5$) dispersed in IPSH matrix ($M_w = 4 \times 10^5$) obtained at different degrees of crystallinity. In *Table 1* are listed the results of the radii of gyration measured for all the investigated samples. For samples of A series one notices a non-negligible increase of R_g while the intercept in the Zimm representation (*Figure 4*) remains constant whatever the crystallinity. This confirms that the scattering species increase in their mean size without any variation of the molecular weight.

Concerning the variation of R_g with molecular weight, this has been plotted in *Figure 5* for $x = 0.3$ and $x = 0$ (previous results available in ref 5) with a logarithmic scale. The classical exponent ν deduced for $x = 0$ is close to 0.5 (characteristic of Gaussian chains) while for $x = 0.3$ one finds $\nu = 0.78$. This last result disagrees entirely with the hypothesis of a semi-crystallized chain behaving globally Gaussian-like.

The study of the scattered intensity in the intermediate range has been carried out both on amorphous and 0.35-crystallized samples containing the same tagged chains ($M_w = 5 \times 10^5$) at the same concentration (C = 0.51%). The data are plotted in *Figure 6* using the Kratky representation $q^2I(q)$. For the two situations the curves reach a plateau, but the values on the ordinate axis are somewhat different. It must be underlined that all the crystallized

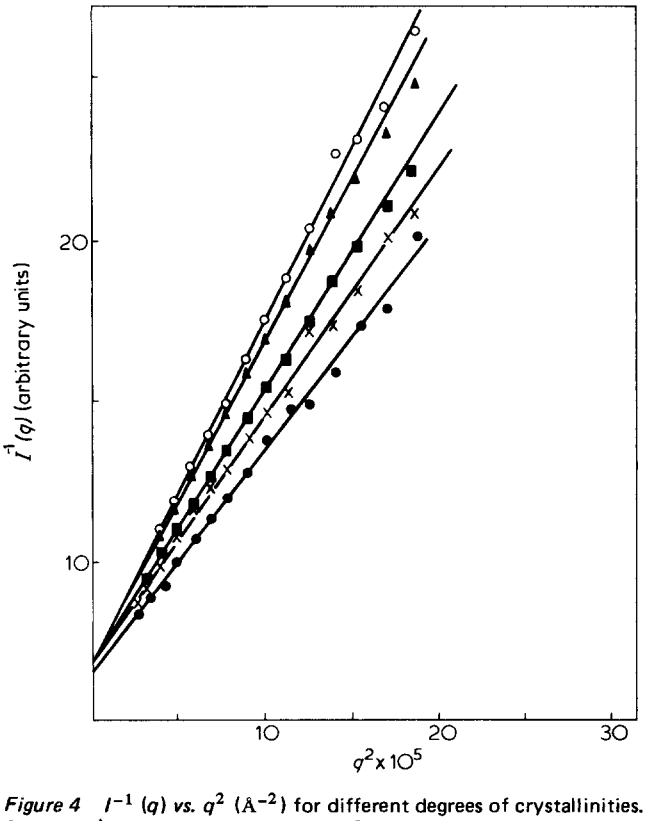

Figure 4 $I^{-1}(q)$ *vs.* q^2 (Å^{-2}) for different degrees of crystallinities. ○ = 0.35, ▲ = 0.3, ■ = 0.25, x = 0.22, ● = 0.16. The slopes are directly related to R_g^2

Table 1 Values of radii of gyration given in Å. The crystalline samples are prepared using an IPSH matrix of weight average molecular weight $M_W = 4 \times 10^5$, while amorphous samples are prepared using an APSH matrix

	M_W/M_n	M_W	x					
			0	0.16	0.22	0.25	0.3	0.35
A	1.2	5×10^5	165 ± 6	180 ± 6	192 ± 11	200 ± 10	210 ± 5	228 ± 10
B	1.2	3×10^5	128 ± 3				144 ± 5	
C	1.15	2.5×10^5	120 ± 2		116 ± 4	120 ± 4	124 ± 3	130 ± 4

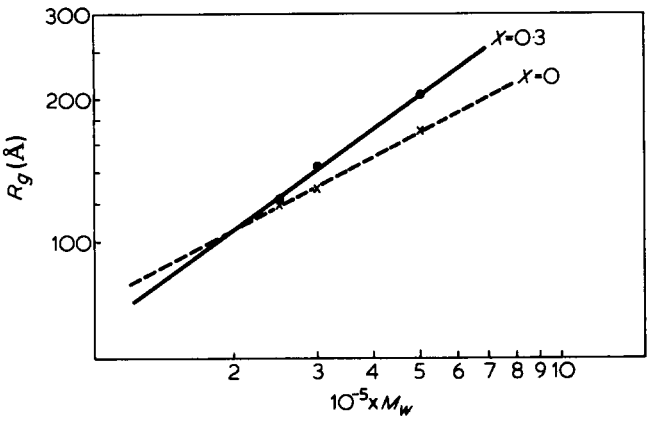

Figure 5 R_g *vs* M_W in logarithmic representation. ●, $x = 0.3$ slope = 0.78; x, $x = 0$ slope = 0.5 (The molecular weights are expressed in hydrogenated equivalent. To obtain the real values one has to multiply by a factor of 1.077)

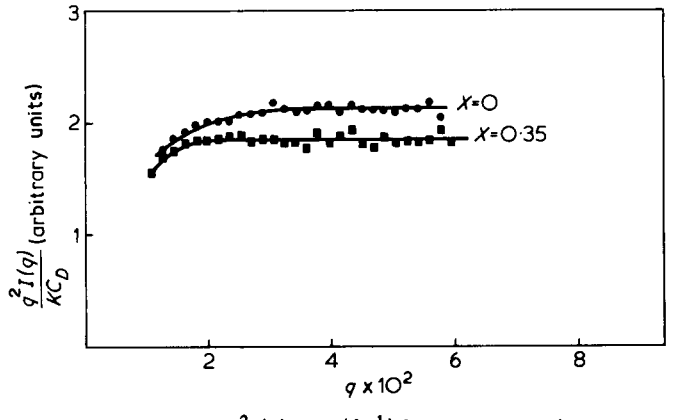

Figure 6 Kratky plot $q^2 I(q)$ vs. q (Å^{-1}) for a pure amorphous sample (●) and a 0.35-crystallized sample (■). Molecular weight and D-species concentration are the same ($M_W = 5 \times 10^5$, $C = 0.51 \times 10^{-2}$ g/ml)

samples exhibit the same behaviour (see for example *Figure 7*). No peak in the Kratky representation has been observed contrarily to annealed polyethylene[8]. Such a peak arises frequently when chains segregate in molecular clusters. These results point out again the non-existence of clustering effect in IPS.

DISCUSSION OF THE EXPERIMENTAL RESULTS

Usually, Flory's model[20] is put forward in order to describe the semi-crystalline chain's conformation for melt-crystallized samples. For labelled macromolecules adopting this shape, one would obtain on the one hand an exponent ν of the law $R_g \sim M^\nu$ close to 0.5 and on the other hand, almost

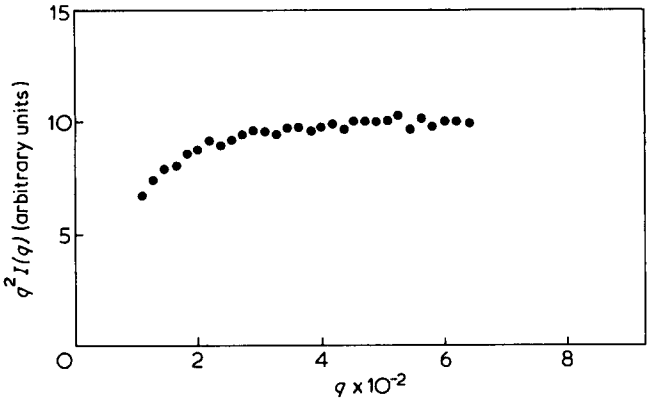

Figure 7 Kratky plot $q^2 I(q)$ *vs.* q (Å^{-1}) for a 0.22-crystallized sample with $M_W = 2.5 \times 10^5$

no variation of the mean dimension with increasing crystallinity. Such results have been observed for melt-crystallized polyethylene which justifies the adoption of Flory's model for this polymer.

From our values of radii of gyration it seems clear that the previous model is inapplicable to the crystalline IPS chains. The increase of the mean dimensions, as well as the exponent $\nu = 0.78$, suggest the use of crystalline chains models having long crystallized sequences for which calculations of the mean dimensions have been developed[21] in the previous paper. It has been particularly demonstrated that a model made of two crystalline sequences and one amorphous sequence (CAC) linked together leads to a comparable result with the Flory-model that considers the invariance of the radius of gyration as crystallinity increases. Consequently, the discussion will be restricted to models having either two sequences (named AC) or three sequences only one of which is crystalline (named ACA).

The plateau observed in the Kratky representation in the intermediate range would denote a unidirectional incorporation of the chain in the monocrystal. This means that the crystalline sequence grows along an (*hkO*) plane of the crystalline lattice (in that case the (110) plane). Then this sequence can be considered sheet-like. By supposing on the other hand amorphous pending chains Gaussian-like one should obtain in the appropriate q range a scattered intensity behaving like $I(q) \sim q^{-2}$. If a and b are respectively the width and the length of the thin sheet this approximation becomes valid only for: $qa > 1$ and $qb > 1$. Then the form factor $P_s(q)$ of a thin sheet reaches the asymptotical expression[22]:

$$P_s(q) = \frac{2\pi}{q^2 ab} \tag{9}$$

On the other hand, by considering the re-entry length l defined in a previous paper[21] as the length between two con-

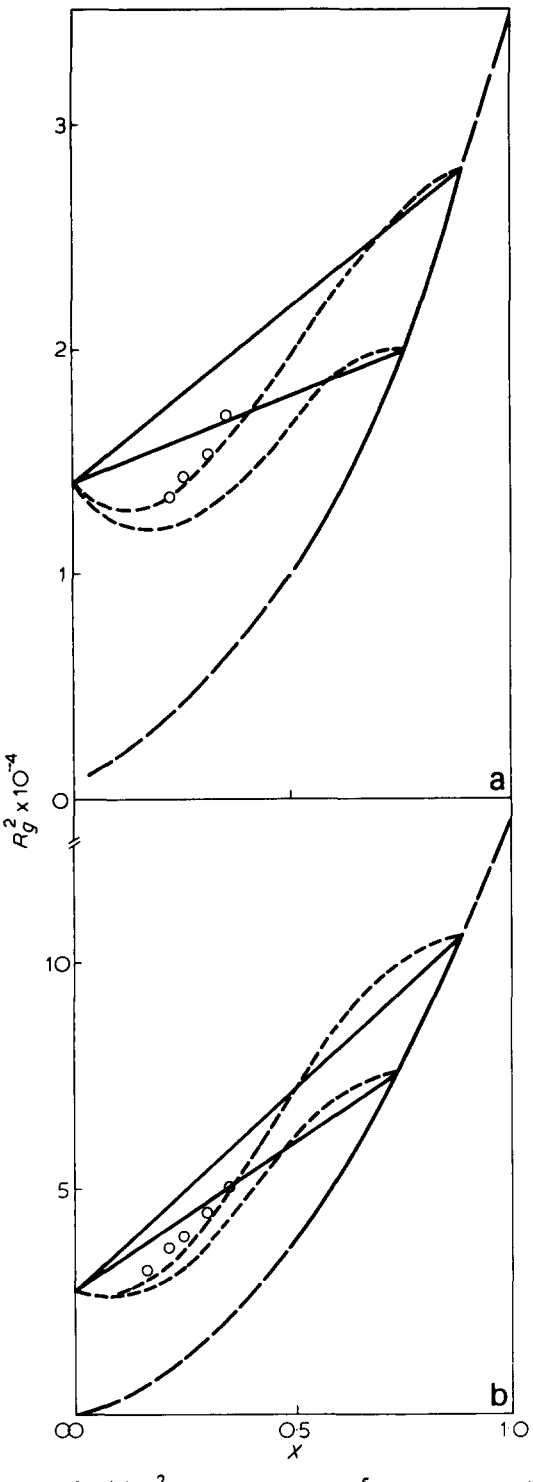

Figure 8 (a) R_g^2 *vs.* $x.M_W = 2.5 \times 10^5$; ——, blend of pure amorphous and totally crystallized chains; — — — —, ACA model. Further explanations of this type of diagram are given in a previous paper[21]. (b) R_g^2 *vs.* $x.M_W = 5 \times 10^5$. Same legend as above.

secutive rods of a tagged chain incorporated in the same monocrystal, relation (9) is suitable only for $qI < 1$, otherwise for $qI > 1$ one would record the contribution of isolated-like rods and moreover Bragg-peaks of the helix configuration.

It appears that the discussion must hereafter be considered in two separate sections. The first will be devoted to the data obtained on the evolution of the mean dimensions and the second to the asymptotic behaviour of the intensity scattered in the intermediate range.

Radii of gyration

It seems necessary, before discussing the data reported in *Table 1*, to recall the relations computed in a previous paper[21] for the AC and ACA models. Namely:
AC model with unidirectional incorporation

$$\overline{R_g^2} = (4 - 3y)y^3 \overline{R_p^2} + y\overline{r_e^2} + (1 - y)^2 (2y + 1)\overline{R_a^2} \qquad (10)$$

ACA model with unidirectional incorporation

$$\overline{R_g^2} = (3 - 2y)y^2 \overline{R_p^2} + y\overline{r_e^2} + \frac{(1 - y)^2}{2} (2 + y)\overline{R_a^2} \qquad (11)$$

where y is the weight fraction of the crystalline sequence, $\overline{R_p^2} + r_e^2$ is the radius of gyration of this sequence for $y = 1$ ($\overline{r_e^2}$ is a term containing the effect of lamellar thickness and loops whereas $\overline{R_p^2}$ is influenced by the trajectory in the monocrystal) and $\overline{R_a^2}$ is the radius of gyration of the considered chain in the complete amorphous state. In these calculations amorphous loops of weight fraction $(1 - z)$ are taken into account in the crystalline sequence. These loops are defined as the amorphous material joining two consecutive rods of the chain incorporated in the same monocrystal. Amorphous material joining consecutive rods on the same chain but incorporated in two different monocrystals is called pending chain (case of CAC model for example). By supposing now that only AC or ACA models are present in the sample and knowing the experimental crystallinity x one would have:

$$y = \frac{x}{z} \qquad (12)$$

Nevertheless, in a semi-crystalline polymer, amorphous domains can always be present especially for weak degrees of crystallinity. Consequently, we have introduced a new set of parameters in order to take into account the different scattering species; namely: w_a the weight fraction of the residual amorphous material unlinked to crystalline sequences; w_c the weight fraction of the amorphous material linked to the crystalline sequences.

These parameters are related in the following way:

$$w_a + w_c + \frac{x}{z} = 1 \qquad (13)$$

with now

$$y = \frac{x/z}{x/z + w_c}$$

We have used a three dimensional diagram to represent such a situation (see previous paper) with w_a, w_c, $\overline{R_g^2}$ as principal axis. However, by plotting $\overline{R_g^2}$ function of x domains can be delimited in which the situations described above are present. Such an array of curves is drawn in *Figure 8*. From these curves it appears that the best agreement corresponds to ACA model. This is particularly marked for the tagged chains of higher molecular weight. For samples with labelled chains $M_w = 2.5 \times 10^5$, the agreement seems good too, but the accuracy of the measurements does not allow us to use such a small variation as an argument in favour of the selected model. On the other hand, these results can correspond also to AC model for samples containing a non-negligible amount of residual

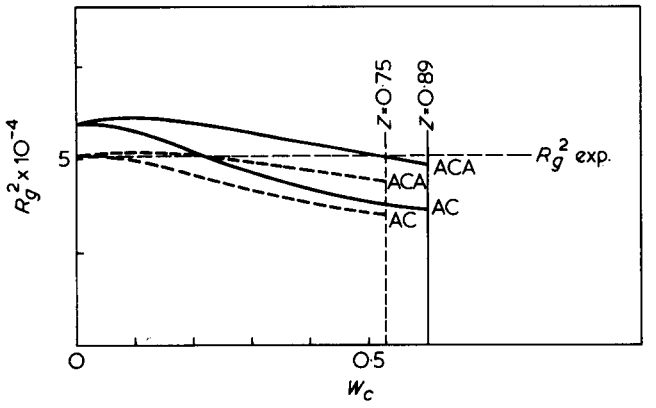

Figure 9 R_g^2 *vs.* w_c for $x = 0.35$. Solid lines represent the variations calculated for AC and ACA models with $z = 0.89$ (tight loops), dotted lines for the same models with $z = 0.75$. – – – –, line gives the experimental value of R_g^2 (see *Table 1*, Series A

Table 2 Values of W_a and W_c obtained from a plot R_g^2 *vs.* w_c at $x = C^{te}$ for different z, and using the experimental values of R_g listed in *Table 1* for $M_{wIPSD} = 5 \times 10^5$

	ACA		AC	
x	$z = 0.89$	$z = 0.75$	$z = 0.89$	$z = 0.75$
0.16	$W_c = 0.45$ $W_a = 0.37$	$W_c = 0.32$ $W_a = 0.46$	$W_c = 0.2$ $W_a = 0.62$	$W_c = 0.16$ $W_a = 0.63$
0.22	$W_c = 0.5$ $W_a = 0.25$	$W_c = 0.33$ $W_a = 0.38$	$W_c = 0.16$ $W_a = 0.59$	$W_c = 0.22$ $W_a = 0.49$
0.25	$W_c = 0.43$ $W_a = 0.29$	$W_c = 0.33$ $W_a = 0.46$	$W_c = 0.2$ $W_a = 0.52$	$W_c = 0.1$ $W_a = 0.57$
0.3	$W_c = 0.54$ $W_a = 0.12$	$W_c = 0.3$ $W_a = 0.3$	$W_c = 0.24$ $W_a = 0.42$	$W_c = 0.14$ $W_a = 0.46$
0.35	$W_c = 0.54$ $W_a = 0.07$	$W_c = 0.23$ $W_a = 0.31$	$W_c = 0.23$ $W_a = 0.31$	$W_c = 0.05$ $W_a = 0.48$

amorphous material. To remove this ambiguity, we try to confirm this last quantity. In *Figure 9* is drawn as example a plot of $\overline{R_g^2}$ as function of w_c for $x = C^{te}$. Knowing the experimental value of $\overline{R_g^2}$, one can then easily determine w_c, w_a, for given x and z. The results are listed in *Table 2* for ACA and AC models. Let us first examine the values obtained for $x = 0.35$. At this degree of crystallinity, optical microscopic pictures do not show any amorphous residual areas. Consequently, the best agreement would be for ACA model with $z = 0.89$. With the other models at $x = 0.35$, $w_a = 0.3$, a value which seems too high compared with the experimental evidence. We choose then the model leading to the weaker amorphous residual material.

Values computed at different x for ACA model with $z = 0.89$ are worth comment. As can be seen in *Table 2* the weight fraction of amorphous residual chains decreases with increasing crystallinity. However, the weight fraction w_c of amorphous linked material remains roughly constant and close to a value corresponding to the linear crystallinity determined by X-ray diffraction.

Finally, to conclude the discussion upon the radius of gyration, we will examine the variation of this quantity with molecular weight. In the case of ACA and AC models, the relation $\log R_g$ as function of $\log M_w$ is not necessarily linear. However, from relations (10) and (11), employing a mean least square method and considering the molecular weights involved in our study (see *Table 1*), one can determine an apparent exponent ν at given x and for different reasonable values of z. From the ν values computed and reported in *Table 3*, it appears that the variation obtained with our data ($\nu = 0.78$) is again in best agreement with ACA model. In return, the value of z cannot be confirmed.

Results obtained on the mean dimensions according all these considerations are relatively well consistent with the ACA model. We will now analyse the scattered intensity in the intermediate range in order to verify the consistency of the model in all the scattering vector domains.

Asymptotical behaviour of the form factor

The form factor has the general expression for non-oriented macromolecules:

$$P(q) = \frac{1}{\sum_i \sum_j \mu_i \mu_j} \left\langle \sum_i \sum_j \mu_i \mu_j \frac{\sin q r_{ij}}{q r_{ij}} \right\rangle \qquad (15)$$

where μ_i and μ_j stand for the contrast factors of i and j elements. For structures of two kinds of scattering centres, the summation can be decomposed in several terms. Before performing the calculation of the form factor, some approximations can be made. The first consists of taking the same contrast for scattering centres whatever their position in the sequences for AC and ACA models. This approximation has been already discussed in the previous paper[21] and seems amply satisfying since densities of the two sequences are close ($d_{cry}/d_{am} \sim 1.06$). The second leads to consider the crystalline sequence to be sheet-like in the range of z values $0.75 \leqslant z \leqslant 0.89$. As the radius of gyration of amorphous loops is rather small in comparison to the lamella thickness in this range of z, the approximation is quite relevant for $qa > 1$ and $qb > 1$ but as previously would be irrelevant for $qI > 1$.

Then $P(q)$ can be written in the case of the two selected models:

$$P_{AC}(q) = \left(\frac{x}{z}\right)^2 P_s(q) + \left(1 - \frac{x}{z}\right)^2 P_{G_{AC}}(q) + (CT)_{AC} \qquad (16)$$

$$P_{ACA}(q) = \left(\frac{x}{z}\right)^2 P_s(q) + \frac{1}{2}\left(1 - \frac{x}{z}\right)^2 P_{G_{ACA}}(q) + (CT)_{ACA} \qquad (17)$$

where subscripts s and G refer respectively to the sheet and to the Gaussian coil. $(CT)_{AC}$ and $(CT)_{ACA}$ are cross-terms

Table 3 Apparent exponents calculated from relations (10) and (11) for different values of z and using a mean least square method with molecular weights reported in *Table 1*

	z	
	0.89	0.75
AC	0.65	0.67
ACA	0.79	0.80

Table 4 Calculated ratio between intensities of pure amorphous and 0.35-crystallized samples. I_{cry} is deduced from relation 20 with l = 12.6 Å

	z	
	0.89	0.75
$\frac{I_{am}}{I_{cry}}$	1.1	1.05

which vanish for wide q. Asymptotic expression of the form factors involved in relations (16) and (17) are:

$$P_s(q) = \frac{2\Pi}{q^2ab} \quad \text{and} \quad P_G(q) = \frac{2}{q^2R_g^2}$$

for wide q, 16 and 17 reduce then to:

$$P_{AC}(q) = \left(\frac{x}{z}\right)^2 \frac{2\Pi}{q^2ab} + \left(1 - \frac{x}{z}\right)^2 \frac{2}{q^2R^2_{G_{AC}}} \qquad (18)$$

$$P_{ACA}(q) = \left(\frac{x}{z}\right)^2 \frac{2\Pi}{q^2ab} + \frac{1}{2}\left(1 - \frac{x}{z}\right)^2 \frac{2}{q^2R^2_{G_{ACA}}} \qquad (19)$$

Moreover, it can be easily demonstrated that the two form factors calculated for AC and ACA structures are identical at wide q leading to:

$$P_{AC}(q) = P_{ACA}(q) = P_B(q) = \frac{x}{z}P_s(q) + \left(1 - \frac{x}{z}\right)P_G(q) \qquad (20)$$

where $P_B(q)$ is the form factor of a blend of pure amorphous chain on the one hand and crystallized chain totally incorporated in the same monocrystal on the other hand.

Then at wide q:

$$P_s(q) = \frac{2\Pi}{q^2ab_T} \qquad (21)$$

$$P_G(q) = \frac{2}{q^2R_a^2} \qquad (22)$$

for which b_T is the length of the thin sheet for a totally crystallized chain and R_a^2 has the same meaning as in relations (10) and (11).

Knowing the form factor of a conformation, the intensity has the general expression:

$$I(q) = KCM_wP(q) \qquad (23)$$

Thereby, experiments already mentioned in *Figure 6*, carried out on samples containing labelled chains of the same molecular weight, can be useful to compare the levels of the plateaux obtained in the Kratky representation. However, by this method we can only verify the presence of a sheet since measurements cannot differentiate the models. Calculations for x = 0 and x = 0.35 for different z are listed in *Table 4*.

From *Figure 6* one deduces the relative ratio between the heights of the plateaux that is:

$$\frac{I_{am}}{I_{cry}} = 1.14$$

For chains adopting a Flory conformation having the experimentally measured radius of gyration R_g = 228 Å, the same ratio should be close to 1.91.

From these data, we confirm therefore the existence of a thin sheet leading to admission of the existence of long crystallized sequences.

DISCUSSION OF THE MODEL

In the discussion, we have tried from our measurements to define a possible conformation for IPS chains in the bulk semi-crystallized state. It appears that the results are consistent with ACA model whatever the explored range of scattering vectors. However, our assumptions depend strongly on the lamellar thickness l_c. Despite the value of 100 Å mostly found for IPS samples annealed at 185°C, we have introduced lower (80 Å) or larger (120 Å) values of l_c in our calculations and compared the new curves to the experimental data. For l_c = 80 Å one finds rather a model closer to CAC conformation whereas for l_c = 120 Å a blend of amorphous chains and totally crystallized chains incorporated into the same monocrystal would be more suitable. Nevertheless, in no case do we find any accord with Flory's model.

By varying the values of l_c we have determined the probable limits of the semi-crystalline chain conformation. The ACA model must be simply considered as a mean conformation. This means that a small fraction of tagged chains could adopt CAC structure or complete crystallized model for instance. Moreover, defects like incorporation of a small portion of the amorphous linked material in another lamella (*Figure 10*) are quite probably leading to the interruption of the crystallinity growth of the chain. Such defect can explain among other explanations the weak crystallinity of IPS.

Neutron scattering results cannot indeed be easily cross-checked with other experiments particularly for crystalline polymers. However some experimental indications show that the deduced model seems to be valid. Recently, Marchal *et al.* have performed dielectric relaxation measurements[23] on IPS samples crystallized following the same procedure as described before. They lead to the conclusion that chain portions located between lamellae are long amorphous sequences. On the other hand, we have followed an idea proposed by Flory and Yoon[24] comparing time scales involved in the crystalline growth rate and relaxation time τ_m of molecules. They find in the case of poly(methylene oxide) that the domain originally occupied by a random coil of 140 Å in the melt is enveloped during an interval of the order of 10^{-2} s while the relaxation time of the same chain is $\tau_m \sim 1$ s. In these circumstances thermal motion of units of the chain can effect only imited arrangements. They conclude that the chain should then remain globally Gaussian-like. In the case of IPS considering the molecular weight of the protonated matrix ($M_w = 4 \times 10^5$), the envelopment time is around 6 s[25] while the relaxation time τ_m is between 5 and 15 s[26]. These quite comparable time scales corroborate the existence of long crystallized sequences. As a consequence, it could be expected that a tagged chain embedded in an IPSH matrix of higher molecular weight than previously should adopt a Flory conformation since long relaxation

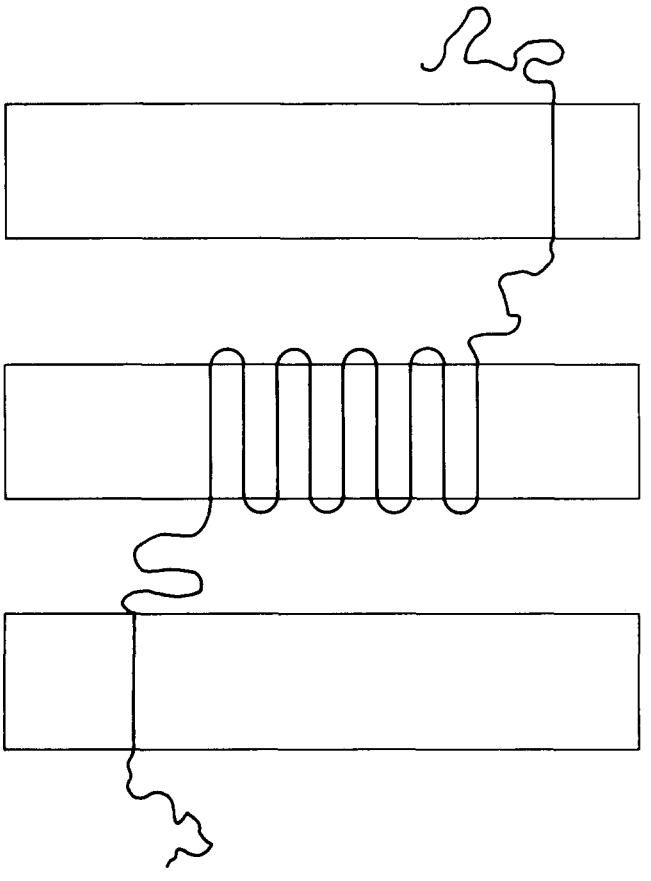

Figure 10 Schematic representation of ACA model showing a type of defect. Small portions of the amorphous linked material are incorporated in different lamellae. This type of defect cannot be differenciated by SANS from a pure ACA model.

Table 5 Values of radii of gyration given in Å. The crystalline samples are prepared using an IPSH matrix of molecular weight $M_W = 1.75 \times 10^6$

		x	
	$M_{W\text{IPSD}}$	0	0.35
D	5×10^5	165	150
E	7×10^5	195	177

time becomes much larger due to the increase of the medium viscosity. In order to conclude, such an experiment has been performed by using an IPSH matrix of weight-average molecular weight $M_w = 1.75 \times 10^6$ for which τ_m is larger than 12 min[26]. The two domains of scattering vectors have been explored for samples crystallized during 50 min at 185°C leading to $x = 0.35$. Values of radius of gyration obtained in the Guinier range are listed in *Table 5*. In this case, one notices only a small decrease of R_g contrarily to the previous experiments for which R_g increases drastically. In the intermediate range of q, data obtained on the crystallized sample of the D series have been plotted in a Kratky representation (*Figure 11*) and compared to the results presented in *Figure 6*. The comparison is justified by the use of the same tagged chains molecular weight. We can see therefore, that for the same degree of crystallinity, the behaviour is quite different. Samples from A and D series for $x = 0.35$ exhibit very different scattering curves shapes in such a plot. If we consider as in the discussion of the experimental results the ratio

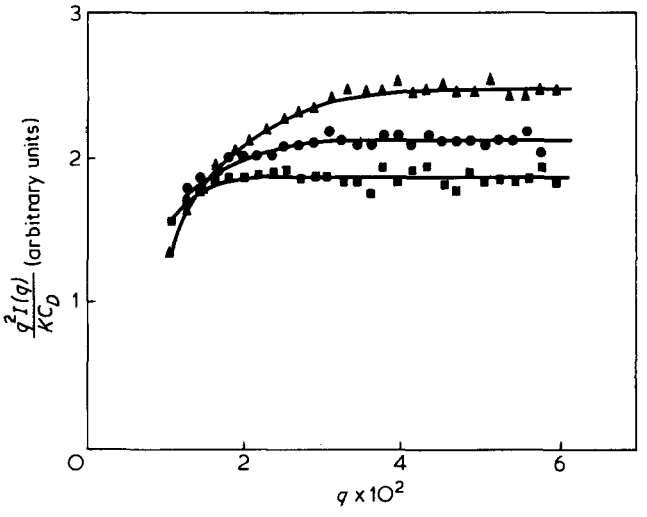

Figure 11 Kratky-plot $q^2 I(q)/KC_D$ vs. $q(\text{Å}^{-1})$ in arbitrary units, ▲, 0.35-crystallized sample in IPSH matrix of molecular weight $M_W = 1.75 \times 10^6$ (From series D); ●, amorphous sample, ■, 0.35-crystallized sample in IPSH matrix of molecular weight $M_W = 4 \times 10^5$ (from series A)

I_{am}/I_{cry} in the case of the sample from D series, (note that amorphous samples in the A and D series are the same) it is close to 0.86 whereas the same ratio calculated for Gaussian chains with respectively $R_g = 165$ Å and $R_g = 150$ Å is 0.83. These considerations support the assumption that for this last situation the labelled chains behave globally Gaussian as revealed both in the Guinier and the intermediate ranges. Small portions of the chains are incorporated in several monocrystals.

CONCLUSION

Finally, all the results described in this paper lead to the following concluding remarks:

(i) The assumption leading to consider large crystallized sequences for samples prepared with the lower molecular weight matrix is confirmed.

(2) They emphasize the great interest of IPS which allows to observe two different chain conformations by only varying the molecular weight of the matrix.

(3) In very polydispersed materials (which is mostly the case for crude IPS), all the chains do not necessarily crystallize with the same conformation.

(4) The comparison between crystallization growth rate and the long relaxation time appears thereafter to be a good criterion to attempt predicting the conformation of the chains in a semicrystalline state for flexible crystallizable polymers.

ACKNOWLEDGEMENT

The authors wish to thank Professor R. Ullman and Professor H. Benoit for helpful discussions, and Dr. R. Duplessix for experimental assistance in Grenoble.

REFERENCES

1 Kirste, R. G., Kruse, W. A. and Schelten, J. *Makromol. Chem.* 1973, **162**, 299; Cotton, J. P. *et al. Macromolecules* 1974, **7**, 863
2 Benoit, H. *et al. J. Polym. Sci. (A2)* 1976, **14**, 2119
3 Daoud, M. *et al. Macromolecules* 1975, **8**, 804

4 Leiser, G., Fischer, E. W. and Ibel, K. *J. Polym. Sci. (C)* 1975, **13**, 39
5 Guenet, J. M., Picot, C. and Benoit, H. *Macromolecules* 1979, **12**, 86
6 Schelten, J., Wignall, G. D., Ballard, D. G. H. and Longman, G.W. *Polymer* 1977, **18**, 1111
7 Allen, G. and Tanaka, T. *Polymer* 1978, **19**, 271
8 Schelten, J., Ballard, D. G. H., Wignall, G. D., Longman, G. and Schmat, W. *Polymer* 1976, **17**, 751
9 Sadler, D. M. and Keller, A. *Macromolecules* 1977, **10**, 1128
10 Yoon, D. Y. and Flory, P. J. *Polymer* 1977, **18**, 509
11 Summerfield, G. C., King, J. S. and Ullman, R. *J. Polym. Sci. (A2)* in press
12 Guenet, J. M., Gallot, Z., Picot, C. and Benoit, H. *J. Appl. Polym. Sci.* 1977, **21**, 2181
13 Natta, G. *J. Polym. Sci.* 1955, **16**, 143
14 Ibel, K. *J. Appl. Crystallog.* 1976, **9**, 296
15 Summerfield, G. C., King, J. S. and Ullman, R. *Macromolecules* in press
16 Overgergh, N., Berghmans, H. and Smets, G. *J. Polym. Sci. (C)* 1972, **38**, 237
17 Overbergh, N., Berghmans, H. and Reynaers, H. *J. Polym. Sci. (A2)* 1976, **14**, 1177
18 Ullman, R. personal communication
19 Bacon, G. E. 'Neutron diffraction', Oxford Edn, 1962; Turchin, V. P. 'Slow neutrons' *Israel Prog. Sc. Trans.* 1965; *M.I.T. Tables* Feb. Apr. (1971)
20 Flory, P. J. 'Principles of polymer chemistry', Cornell University Press, Ithaca, 1967
21 Guenet, J. M. and Picot, C. 1979, **20**, 1473
22 Guinier, A. and Fournet, G. 'Small angle scattering of X-rays, Chapman and Hall, London, 1955
23 Marchal, E., Vogl, O. and Benoit, H. *J. Polym. Sci. (A2)* 1978, **16**, 949
24 Flory, P. J. and Yoon, D. Y. *Nature* 1978, **272**, 226
25 Picot, C. *Thesis* Strasbourg (1968)
26 Suzuki, R. *Thesis* Strasbourg (1972)